이학박사 학위논문

생쥐 전대상피질의 가려움 및 고통 신경 네트워크에 대한 시스템적 연구

Systematic studies on the neuronal network of itch and pain ensembles in the mouse anterior cingulate cortex

2023년 8월

서울대학교 대학원

뇌과학협동과정

이 치 우

생쥐 전대상피질의 가려움 및 고통 신경 네트워크에 대한 시스템적 연구

지도 교수: 강 봉 균

이 논문을 이학 박사 학위논문으로 제출함

2023년 6월

서울대학교 대학원
뇌과학협동과정 (뇌과학 전공)
이 치 우

이치우의 이학 박사 학위논문을 인준함
2023년 6월

위원장 김 형

부위원장 강 봉 균

위 원 이 용 석

위 원 고 형 곤

위 원 이 재 형

Systematic studies on the neuronal network of itch and pain ensembles in the mouse anterior cingulate cortex

Advisor: Bong-Kiun Kaang

Submitting a Ph.D. Dissertation of
Brain Science

June 2023

Graduate School of Interdisciplinary Program in Neuroscience of Seoul National University
Brain Science Major

Chiwoo Lee

Confirming the Ph.D. Dissertation written by
Chiwoo Lee

June 2023

Chair	Hyoung F Kim
Vice Chair	Bong-Kiun Kaan
Examiner	Yong-Seok Lee
Examiner	Hyoung-Gon Ko
Examiner	Jae-Hyung Lee

ABSTRACT

Systematic studies on the neuronal network of itch and pain ensembles in the mouse anterior cingulate cortex

Chiwoo Lee

Interdisciplinary Program in Neuroscience

College of Natural Sciences

Seoul National University

The circuits and mechanisms of itch and pain have been studied primarily in receptors and ganglia in the peripheral nervous system and are closely related, but relatively little is known about how these two stimuli are differentiated and influence each other in the central nervous system. The anterior cingulate cortex is a brain region known to process itch and pain sensations, but their interactions are not well understood. In this study, I looked at 1-photon calcium imaging of the anterior cingulate cortex during drug-induced itch and pain. I first identified the time dependence of neuronal populations labeling itch and pain, and analyzed neural firing

patterns based on power spectral density analysis, which showed that the anterior cingulate cortex had distinct firing patterns in response to itch and pain stimuli. The network analysis results suggest the existence of time-dependent functional hubs during pain or itch responses processed in the anterior cingulate cortex. The present study revealed the existence of two neuronal populations representing itch and pain processing.

Keyword : itch, pain, calcium imaging

Student Number : 2017-29201

Table of Contents

Chapter 1. Introduction.....1

Chapter 2. Calcium image shows pain/itch has its own population ...12

Chapter 3. Itch and pain signal distinguished by using ML classifier 21

Chapter 4. Itch and pain have their own network structure 27

Chapter 5. Behavior data shows scratching has distinct response 33

Chapter 6. Conclusion 37

References.....41

Abstract in Korean 47

List of Figures

Figure 1. Data acquisition and processing steps.....15

Figure 2. Overlapping % of itch and pain ensembles.....16

Figure 3. PSD(power spectral density) analysis implies itch and pain's controversial relationship 18

Figure 4. Shannon entropy shows stimuli induces increase of Shannon entropy. FFF, HHH, FHF, HFH. 19

Figure 5. Machine learning classification process and classification matrix26

Figure 6. Physical distance and itch network property 31

Figure 7. Network property of itch and pain network, compared with scrambled data. 31

Figure 8. Network metric comparison. Small worldness difference showed pain network is affected by drug stimuli.....32

Figure 9. Time window shows pre-post Δcalcium signal efficiently.....37

Chapter 1.

Introduction

Backgrounds

Itch and pain, two multifaceted sensations, have been subject to extensive scientific investigation over the years. These sensations play a crucial role in the everyday experiences of animals, acting as warning signals that help protect organisms from potential harm. Pain is an aversive sensation that alerts the body to potential tissue damage, while itch serves to signal the presence of irritants or parasites on the skin.

Both itch and pain processing rely on intricate neural networks that span from the periphery to the central nervous system. These networks enable the rapid detection and transmission of noxious stimuli, ensuring that an organism can respond appropriately to environmental threats. In the context of survival, pain processing is essential in safeguarding the physical integrity of an organism. It enables the identification of harmful stimuli, allowing for the initiation of withdrawal reflexes, and promotes learning to avoid potentially damaging situations in the future. Similarly, itch processing is critical in maintaining the health of the skin, the body's largest organ and primary barrier against infection and environmental hazards. By inducing a scratching response, itch processing facilitates the removal of irritants, allergens, or parasites from the skin, thereby preserving its integrity and function.

The importance of these protective mechanisms becomes especially evident when considering the consequences of their dysfunction. Chronic pain and itch conditions, resulting from maladaptive changes in the nervous system, can significantly impair an individual's quality of life and pose a substantial burden on

healthcare systems. Furthermore, the inability to experience pain or itch due to congenital insensitivity can lead to severe tissue damage, infection, and even death, underscoring the significance of these sensations for survival.

Despite sharing some overlapping neural pathways, itch and pain are distinct sensations that can be differentially modulated at the receptor and brain levels. There are several main theories to explain this multifaceted relationship. The main concepts were the transition from itch to pain according to increased nociceptors' discharge frequency (intensity theory; Frey, 1922), encoding of itch and pain by various discharge patterns composed in the central nervous system (pattern theory), and specific separate pathways for itch and pain (specificity theory). For instance, at least one algogen, such as capsaicin, also excites histamine-responsive fibers. In this case, one can question the specificity of the mediator (Namer et al., 2008) or the specificity of the fibers (McMahon and Koltzenburg, 1992).

Not only acute itch/pain but also chronic itch/pain relationship have many similarities and differences. (10) They share some mediators and related receptors, but some work in opposite ways. (11-13) For example, capsaicin, heat, and low pH can induce itch and pain with their common receptor, TRPV1. However, in the case of some opioids like μ-opioid and κ-opioid, they induce itch but suppress pain.

Both pain and itch information enter the thalamus via the spinothalamic tract after leaving the spinal cord and are transmitted to other brain regions, which are involved in processing and modulating these signals. The anterior cingulate cortex (ACC) is a critical region in the processing of affective and cognitive aspects of pain, and recent evidence has implicated its role in itch processing as well. The ACC receives inputs from the spinal cord and other brain areas, such as the

thalamus and insular cortex, and integrates these signals to mediate the emotional and attentional components of itch and pain experiences.

To elucidate the dynamic relationship between sensory information processing and neural ensembles, it is important to how neural populations react to sensations. To observe ACC neuron's activity and their dynamics in freely moving mice, I used activity-sensing fluorescent indicators, especially calcium indicators, GCaMP. To observe this GECI fluorescent signals, Miniscope is used, which is a miniature, head-mounted fluorescent microendoscope, weighing approximately 3 grams. It is based on the principle of wide-field epifluorescence microscopy and is equipped with a complementary metal-oxide-semiconductor (CMOS) sensor for image acquisition. By using these techniques, I could classify the activities of cells as a form of fluorescent signals.

Despite pain and itch's ubiquity, the complex mechanisms underpinning these sensations and their significance in survival are still not fully understood. This paper aims to provide a comprehensive overview of the current understanding of itch and pain processing in mice at brain levels, with a particular focus on the role of the ACC. I will discuss the functional significance of the ACC in mediating the affective and cognitive aspects of itch and pain experiences and discuss the potential implications.

Experimental procedure

Animal

Fos-tTA x tetO-H2BGFP transgenic mice were generated by crossing Fos-

tTA+/- with tetO-H2BGFP+/-. 8~10-week old of Fos-tTA x tetO-H2BGFP and Fos-tTA mice were used for the molecular experiments. Miniscope experiments were performed with 8~10-week old male C57BL/6N mice, and their ACC neurons were recorded at age 14~16 weeks. All mice were housed in a 12-hr light/dark cycle in standard laboratory cages and given ad libitum access to food and water. Fos-tTA x tetO-H2BGFP and Fos-tTA mice were exceptionally provided with doxycycline pellets (40g/kg) since they were born and subsequently changed to standard food pellets during dox-off periods. All procedures and animal care followed the regulation and guidelines of the Institutional Animal Care and Use Committees (IACUC) of Seoul National University.

Formalin and histamine injection

1% formalin solution and 40mM histamine solution were always made freshly on the day of injection. Both solutions were diluted with saline and injected with different Hamilton syringes. Mice were anesthetized with isoflurane and shaved in the back of the neck with an electric razor one day before the first injection. On the day of injection, mice were anesthetized with ketamine/xylazine mixture and injected with 10λ of 1% formalin solution or 20λ of 40mM histamine solution. Formalin solution was injected at the hind paw, and histamine solution was delivered by intradermal injection at the back of the neck.

Experimental procedure with Fos-tTA x tetO-H2BGFP mice

Mice were habituated to handling for 7 days before the first injection. During the last 4 days of habituation, standard food pellets without doxycycline were

provided to all mice and changed to doxycycline pellets again after the histamine injection. Histamine was injected after anesthetizing with isoflurane. Mice were injected formalin with 6h or 72h interval. After 90 min from the formalin injection, they were perfused for immunohistochemistry.

Experimental procedure with Fos-tTA mice

AAV1-tetO-hM4Di-P2A-emGFP was injected bilaterally into ACCs (AP +0.7 mm, ML ±0.4 mm, DV −1.7 mm) by stereotaxic surgery (Stoelting Co.). The mice were given 14 days to recover after stereotaxic surgery. One week after the stereotaxic surgery, mice were habituated to handling for 7 days. During the last 4 days of the recovery period, standard food pellets without doxycycline were provided to all the mice. CNO (clozapine-N-oxide) (10mg/kg) or saline as a vehicle was delivered by intraperitoneal injection 30 min before the second injection. For testing the inhibition of itch behavioral response, formalin was injected into one mice group, and histamine was injected into the other mice group as the first injection. Histamine was delivered to all mice as the second injection, and the scratching behaviors were recorded for 30 min for bouts counting. For testing the inhibition of pain behavioral response, one group of mice was injected with formalin and the other group with histamine as the first injection. All mice were injected with formalin as the second injection, and the hind paw licking behaviors were recorded for 1 hour for counting the duration of licking behavior.

Immunohistochemistry

Mice were anesthetized and transcardially perfused with PBS (0.1 M

phosphate buffer, pH 7.4) followed by 4% paraformaldehyde (PFA) in PBS. Brains were collected and immersion-fixed with 4% PFA at 4°C overnight, cryo-protected with 30% sucrose in PBS for two days at 4°C, embedded in an OCT (optimum cutting temperature) compound (Tissue-Tek, Sakura Finetechnical). Coronal sections (40 μm thick) were made using a cryostat, and every 4th section was collected in 50% Glycerol in PBS. Sections were washed with PBS for 5 min three times, incubated with a blocking solution (PBS containing 10% normal goat serum and 0.3% Triton X-100) for 30 min at room temperature, and incubated with rabbit anti-c-Fos antibody (1:250, Santacruz) diluted in the blocking solution for two days at 4°C. Sections were washed with PBS containing 0.3% Triton X-100 (PBST) for 10 min four times, incubated with fluorescent-conjugated secondary antibodies (1:500) diluted in the blocking solution for 2 hours at room temperature, washed with PBST for 10 min four times. After sections were incubated with DAPI (0.2 μg/ml, Invitrogen) in PBS for 10 min at room temperature, sections were transferred onto glass slides and mounted with VECTASHIELD (Vector Laboratories). The sections were imaged with an LSM700 (Carl Zeiss) confocal microscope, and the images were analyzed using IMARIS software.

Integrated microendoscope

For in vivo 1-photon calcium imaging, I made use of integrated microendoscopes, called miniscopes. The miniscope V3 was used for the experiments. A CMOS imaging sensor (Aptina, MT9V032) was printed on a CMOS imaging sensor PCB, while it was connected to a coaxial cable (RG-174/U(50Ω)) by soldering. Luxeon SMD blue LED (P/N LXML-PB01-0030), soldered

with excitation LED PCB (printed circuit board), was integrated into the main body structure with CMOS imaging sensor PCB. As optic tools, 5mm Dia. x 12.5mm FL, MgF2 Coated, Achromatic Doublet Lens (Edmund Optics, 49-923), Excitation filter (Chroma, ET470/40×), Emission filter (Chroma, ET525/50m), Dichroic mirror (Chroma, T495lpxr) were also integrated to the main body of the miniscope. 3.0-mm diameter N-BK7 half-ball lens (Edmund Optics, 47-269) was glued with optical adhesive (Edmond Optics, 55-084) and cured by UV. Integrated miniscope was linked to the commutator (PANLINK, PSR-C6) which prevented the coiling of cable.

Stereotaxic surgeries for calcium imaging

For virus injection surgery, mice (8~10 weeks) were anesthetized by intraperitoneal injection of ketamine/xylazine solution and placed on a stereotaxic apparatus (Stoelting Co.). AAV2/1-Ef1α-GCaMP6f was injected into the right ACC (AP +0.7mm, ML +0.25mm, DV -1.9mm) using a 33-gauge needle with Hamilton syringe. 2 min after the needle tip was placed on 0.1mm below the target location, it returned to the target location and injected 0.5μl of the virus with 0.125μl/min of injection speed. The needle was pulled out slowly 7 min after the injection finished. One week after AAV injection, GRIN lens (graded-index lens) with 2.0mm in diameter (Go!Foton, CLHS200GFT027) was implanted over the ACC. Mice were anesthetized by intraperitoneal injection of ketamine/xylazine solution and positioned in a stereotactic apparatus. The craniotomy for the GRIN lens was 2.0~2.1 mm in diameter so that the gap between the GRIN lens and skull was not almost existed. A cylindrical column of the neocortex was aspirated until the plane

that subfornical artery was located with a DNA loading tip flowing saline with a blunt 10ml syringe. After the bleeding stopped, a blood clot was gently removed, and the GRIN lens was implanted (DV 1.7mm) into the hole. The skull was additionally screwed up for structural support. The GRIN lens and screws were fixed with Loctite and dental cement. After curing, biocompatible Silastic elastomer (Kwik-Sil, World Precision Instruments, Berlin Germany) was added around the GRIN lens for protection from scratch. Three weeks after the GRIN lens implant surgery, mice were anesthetized by intraperitoneal injection of ketamine/ xylazine solution and positioned in a stereotactic apparatus for a baseplating operation. A baseplate, attached to a miniscope, was placed on the GRIN lens and fixed with dental cement at the angle where the GCaMP6f signal was shown best. The GRIN lens was covered by a cap with screwing on baseplate until the day of calcium imaging.

Miniscope habituation procedures

C57BL/6N mice which underwent whole stereotaxic surgeries were monitored for one week after the baseplating operation. Mice were housed individually in a single cage, and all training and testing were conducted during the light cycle. The mice were habituated to cap removal and miniscope attachment for 5 days without isoflurane anesthesia. Each habituation step endured for 10 minutes after 30 min resting in a rack, and one miniscope was used for one mouse. After habituation to handling during first 2 days, mice underwent miniscope attachment habituation for 2 days, in which miniscopes were attached to baseplates on mice's head with screws and mice were delivered to a new cage and freely moved for 30 sec and

miniscopes were detached again and mice were given to the cage and freely moved for 30 sec. This procedure was repeated for 10 min. In the last day of habituation, mice were habituated to an anesthesia box by moving from a cage and an anesthesia box in every 30 sec.

Calcium imaging of freely moving mice

On the day of calcium imaging, mice were rested at a rack for 30 min with attaching a miniscope linked with a commutator. Calcium imaging was performed during the light cycle, and calcium events were recorded by DAQ software (available at https://github.com/daharoni/Miniscope_DAQ_Software) at 30 frames/s of frame rates and with the maximum gain of CMOS sensor. For preventing photobleaching events, LED power was given between 3~10%, and the LED was turned off except for the imaging steps. Each mouse got the constant LED power during three imaging sessions (0h, 72h, 78h). The commutators were connected to the DAQ board to send the signal from the CMOS to the software on a computer. Before each injection, basal states of neuronal activities were recorded for the first 5 min. Mice were anesthetized with isoflurane and injected histamine into the subcutaneous tissues of the nape neck or formalin into the subcutaneous tissues of the hind paw. After 5-min recovery from isoflurane, calcium signals of itch or pain behavioral responses were imaged for 10 min. After calcium imaging, mice were detached their miniscopes, attached their caps again, and went back to the home racks. In this manner, the three calcium imaging sessions were repeated for one mouse.

Data acquisition, processing, and cell sorting of calcium imaging

The video of calcium transients captured by DAQ software and DAQ hardware (Labmaker or Sierra Circuits, v3.2) were saved as AVI file extension formats. Those videos were processed by CaImAn program, which is the open-source library for calcium imaging data analysis based on the CNMF algorithm (Giovannucci et al., 2019). Initially, movies of each session were integrated into a single video. The integrated videos went through several analyzing steps, including pre-processing and neural activity identification. Pre-processing consisted of 3 steps: motion correction, source extraction, and activity deconvolution.

Chapter 2.

Itch and pain have distinct population in calcium imaging

Introduction

Previous studies have largely relied on electrophysiological recordings or post-mortem analyses to investigate neuron activity. However, these approaches have limitations, including limited spatial resolution, invasiveness, and the inability to observe neuronal activity in real-time in freely moving animals.

In this paper, I used the UCLA Miniscope—a miniature, head-mounted fluorescence microscope weighing approximately 3 grams—for overcoming these limitations and investigate *in-vivo* observation of ACC neuron activity. ACC neurons' real-time activity are imaged by optimized Miniscope. The mice were separated into four groups based on the sequence of drugs they were injected with: 1) the H-H-H group, 2) the formalin-formalin-formalin (F-F-F) group, 3) the histamine-formalin-histamine (H-F-H) group, and 4) the formalin-histamine-formalin (F-H-F) group. (Fig 1)

Following the identification of neurons within calcium imaging data, the degree of overlap among co-activated cells across various experimental sessions was quantitatively assessed. The findings indicate that the homologous-homologous (H-H) sequence group remains unaffected by the presence of temporal gaps, in contrast to the homologous-foreign (H-F) sequence group. Employing this analytical framework allowed for the precise delineation of activated cells and the characterization of individual signaling events within the neuronal population (Fig 2)

The initial pair of stimuli were administered with a 6-hour interval, while the third stimulus was delivered 72 hours subsequent to the second stimulus. Prior to

imaging, a five-day habituation process with miniscopes was carried out in order to mitigate the potential impact of isoflurane anesthesia and minimize recovery time. Neuronal activities in both the basal state and in response to formalin or histamine were imaged and subsequently analyzed using the Min1pipe software.

To calculate the overlapping percentage of co-activated cells across sessions, detected cells from every two sessions were aligned. Cells with matching location coordinates were considered to be overlapping and treated as corresponding cells.

Results

Results indicating that overlapping rates were higher for the 6-hour interval compared to the 72-hour interval. A comparison was made between the ratio of overlapping rates at 6-hour and 72-hour intervals and the ratio of overlapping rates at 6-hour and 72-hour intervals in the basal state, which served as a proxy for endogenous excitability cycles in the anterior cingulate cortex (ACC) region. None of the groups demonstrated a significant deviation from chance level, suggesting a tendency for ACC neurons to be influenced by excitability.

These findings are in accordance with prior research and provide evidence that data acquired through miniscope imaging can corroborate results obtained from transgenic mice and immunohistochemistry (IHC) data.

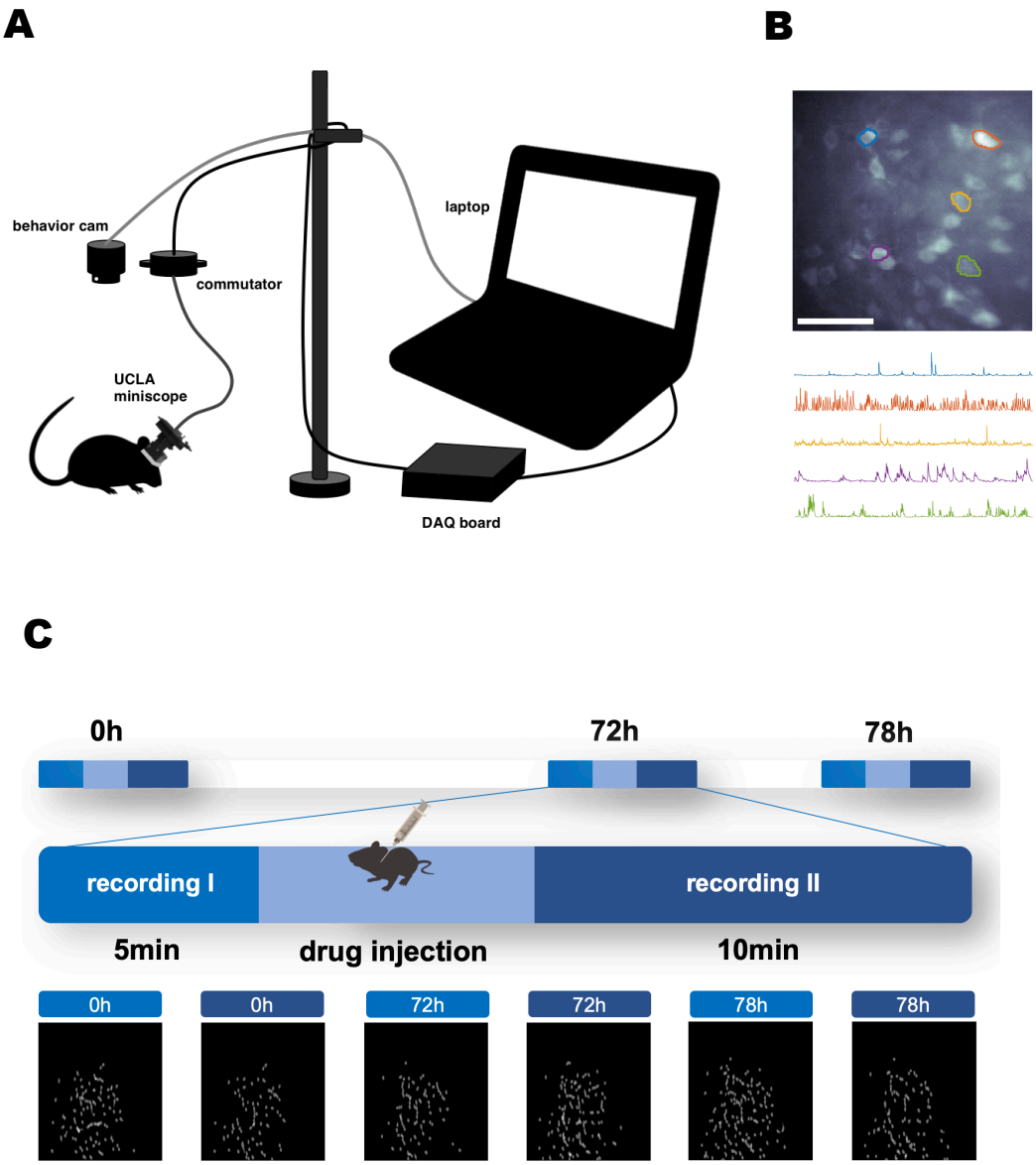

Figure 1. Data acquisition and processing steps

(a) Experiment environment. Freely moving mice's behavior and calcium signal recorded simultaneously. (b) Experiment design and representative spatial footprint. drug: H(histamine) or F(formalin). group: HHH, FFF, HFH, FHF for each timeline. (c) calcium signal from microendoscope recording. bar size: 100um

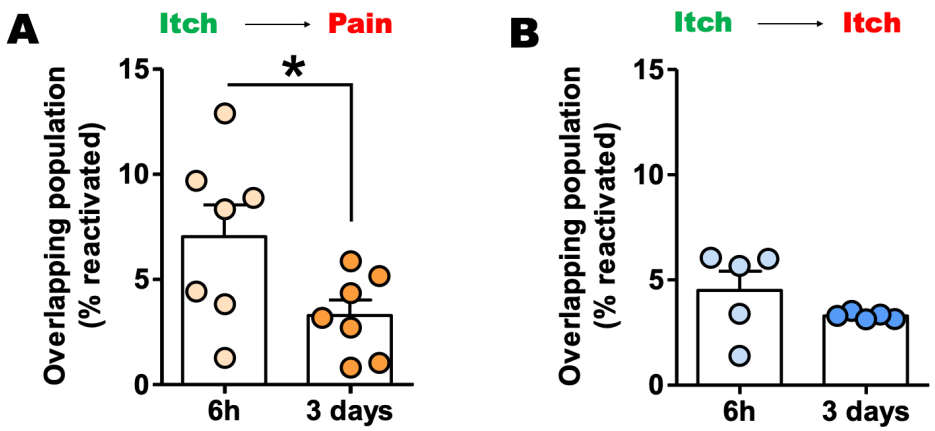

Figure 2. Overlapping % of itch and pain ensembles

(a) itch-pain overlap % (b) itch-itch overlap %. Overlapping % compared from the different time apart condition.

Next, an investigation was conducted to determine whether the recorded signals contained distinct frequency components, utilizing power spectral density (PSD) analysis. Figure 3 reveals a significant difference in the power spectral density between the itch and pain groups. Additionally, Figure presents itch and pain PSD data at three time points, indicating that itch and pain exhibit unique PSD distribution ranges. However, it is noteworthy that the initial chronic itch and final chronic pain exhibited similar PSD distribution patterns. In the homologous-foreign (FHF) group, a single neuron was tracked throughout the entire timeline. Intriguingly, this neuron's signal was found to be analogous to those of other pain/ itch-responsive cells. Nevertheless, the administration of a pain stimulus within 6 hours of the itch stimulus resulted in fluctuations in this distribution. Observation implies that the process of itch-pain signal integration and topological categorization may necessitate a period of more than 6 hours for completion.

a

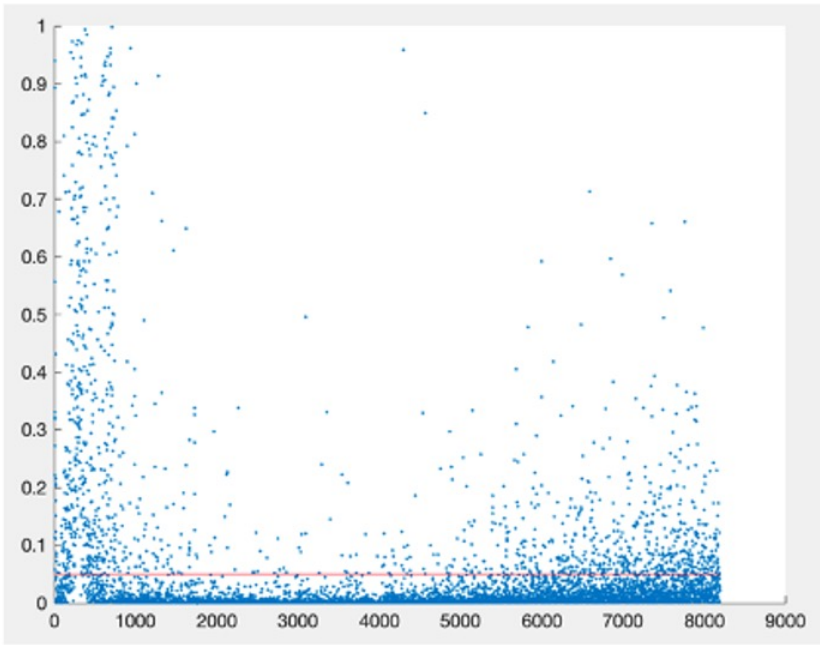
Significance: H - F power distribution
1
0.9
0.8
0.7
0.6
0.5
0.4
0.3
0.2
0.1
0
0
1000
2000
3000
4000
5000
6000
7000
8000
9000

b

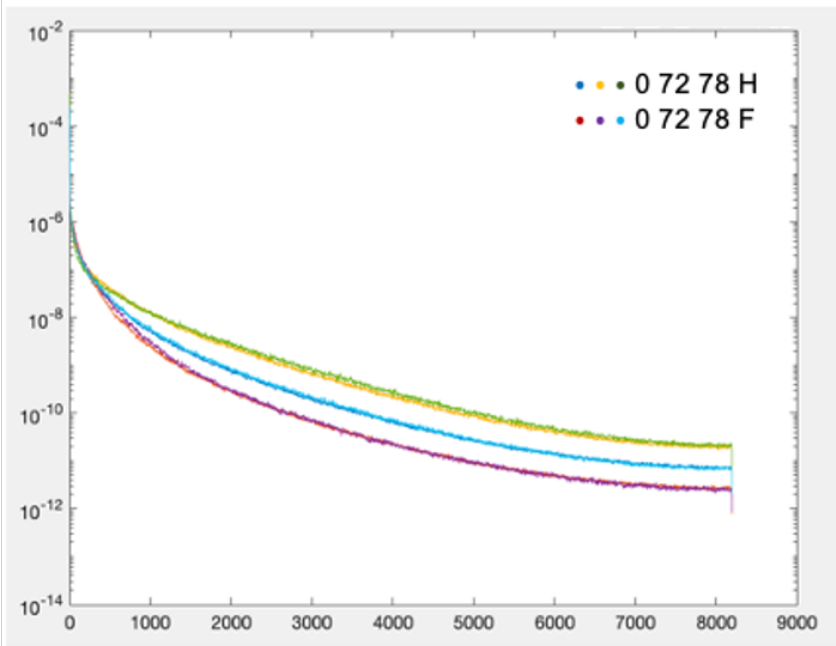
HHH vs FFF
0 72 78 H
0 72 78 F
10^-2
10^-4
10^-6
10^-8
10^-10
10^-12
10^-14
0
1000
2000
3000
4000
5000
6000
7000
8000
9000

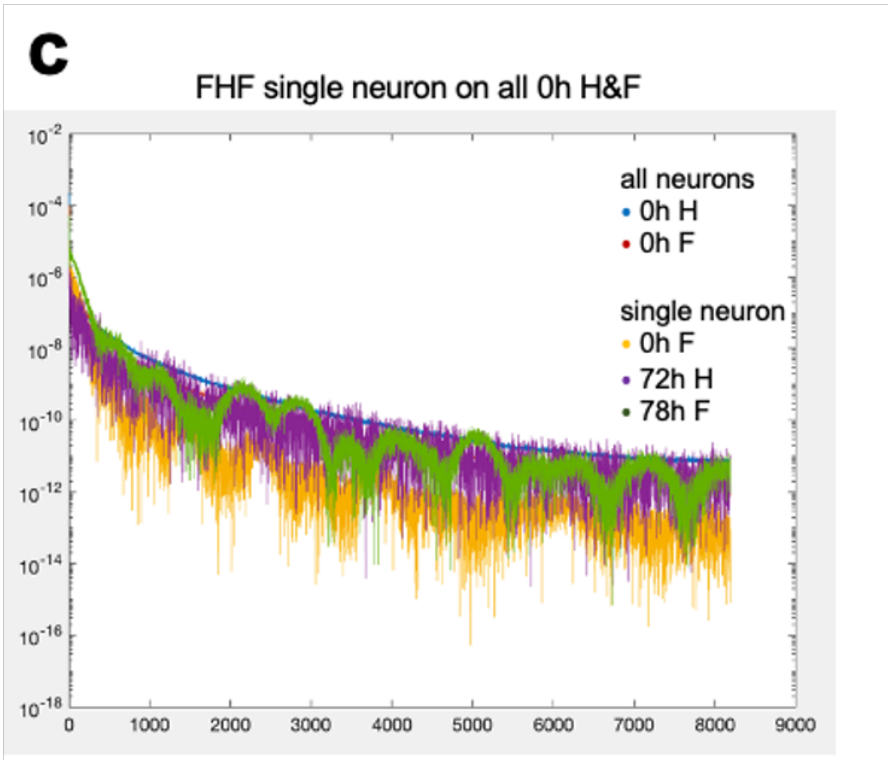

Figure 3. PSD(power spectral density) analysis implies itch and pain's controversial relationship

(a)~(c) x axis: binned frequency(0~8193 means 0~7.5Hz), y axis: amplitude/freq(log scaled for fig b and c) (a) Power distribution comparison. H and F frequency factor can be distinguished around 0.9~5.5Hz. ANOVA for each frequency, 8193 times in total. Red line indicates p-value=0.05 (b) PSD distribution tested on 6 conditions, converged on 3 bands. First and last band are used for pain/itch independently but middle band shared. (c) FHF single neuron shows fluctuation between itch/pain band.

A

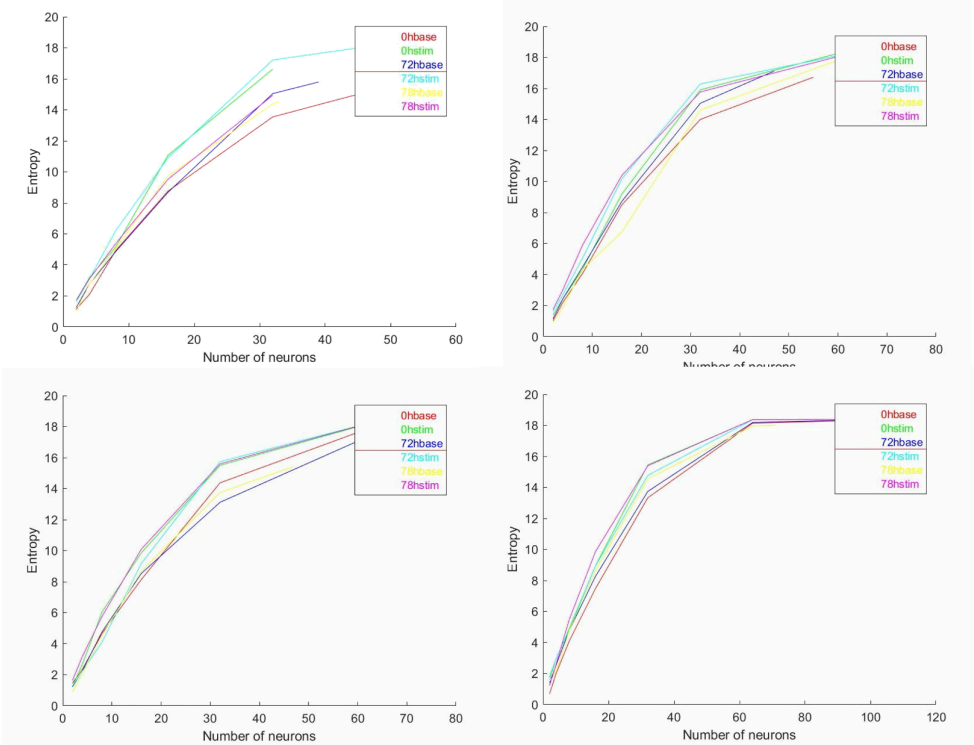

Figure 4. Shannon entropy shows stimuli induces increase of Shannon entropy. FFF, HHH, FHF, HFH.

(a) Stimuli group always have higher Shannon entropy, compare to the baseline group

Statistically, Shannon entropy refers to the degree of randomness in calcium signal intensity (brightness). From a biological perspective, this can be interpreted to mean that as the complexity of information processing increases, entropy also increases. Consistency in this analysis was observed (Fig 4), with the stimulated group consistently exhibiting higher entropy values than the control group. In other words, during information processing, whether in response to pain or itch, the neuronal network experiences a greater load compared to its baseline state

(control).

Interestingly, in the homologous (FFF, HHH) groups, entropy was found to either decrease or remain similar as stimulation was repeated. Specifically, in the FFF group, entropy decreased with each successive stimulus. Conversely, in the heterologous (FHF, HFH) groups, entropy increased with repeated stimulation. This suggests that repetitive and predictable stimuli, whether pain or itch, do not necessitate complex processing, resulting in similar or decreased entropy values. However, when the stimuli are less predictable (less repeated), entropy values either remain similar or increase, reflecting the higher degree of processing complexity required.

Chapter 3.

Itch and pain have distinct population in calcium imaging

IntroductionChapter 3. Itch and pain signal distinguished by using machine learning classifier

In recent years, there has been growing interest in understanding the mechanisms underlying itch and pain, as well as their distinction at the neural level. Machine learning techniques have emerged as powerful tools for the analysis of complex datasets, providing new insights into various aspects of neuroscience. In this paper, I explore the use of machine learning classifiers to distinguish between itch and pain signals based on neural activity patterns.

While many AI algorithms are used to analyze data in this way, I used traditional, mathematical methods to minimize distortions in data interpretation. Essentially, I used the data after deconvolution, rather than a representative value such as the total amount or average of activity. Due to the nature of calcium imaging data, the majority of analyses are conducted based on the intensity of neuronal activity itself. It is possible to detect firing peaks and calculate frequency from the obtained data; however, due to the temporal resolution of genetically encoded calcium indicators (GECIs), these peaks do not necessarily represent individual neuron action potentials, which imposes certain limitations. Instead of relying on firing peak frequency, we aimed to distinguish neural population responses to stimuli at the population level by analyzing activity patterns or distributions, and we sought to employ artificial intelligence (AI) for this purpose.

One inherent limitation from the outset was that calcium imaging data is difficult to directly compare with data from time resolution-focused studies, such as

in-vivo recordings. As a result, it was anticipated that determining whether there are differences in neural population responses or identifying the origins of any such differences would be challenging. To overcome this, we aimed to assess whether neuron population responses to pain and itch stimuli were consistently distinguishable across various AI algorithms. Additionally, we sought to select a model with minimal bias for use in our research. For this purpose, we considered only mathematical models with established reproducibility, albeit potentially limited performance, that have been traditionally employed.

During the training and validation stages, I conducted analyses based on Weka program code. As the overall number of neurons was sufficient, I opted for 10-fold cross-validation to increase the reliability of our analysis. In the visualization process, instead of using receiver operating characteristic (ROC) curves, which typically display individual algorithm performance, I employed neuron-based confusion matrices due to our research objective of signal classification. The rows of the confusion matrix represent input, i.e., the data classified during the experimental stage, while the columns represent output, meaning the results classified by the AI classifier in an unlabeled state. This approach aimed to provide an intuitive representation of how the actual data was classified by the AI algorithm.

I trained classical SMO classifier to distinguish between itch and pain signals, using the Weka program, an open-source suite of machine learning software. This platform was chosen due to its capability to handle large datasets, its versatility, and its accessible and user-friendly interface. The algorithm was used to construct a support vector machine (SVM) model that predicted neuronal activation patterns based on the calcium imaging data.

Trained ML's performance was verified through confusion matrix. An overview of the process is described in the figure, and the confusion matrix is a visualization of the results. The SMO classifier demonstrated high performance in distinguishing between itch and pain signals in mouse calcium imaging data. The confusion matrix revealed that the SVM classifier. The majority of misclassifications occurred as false negatives for itch signals and false positives for pain signals.'

To quantify the performance of the SMO algorithm, a confusion matrix was used. This tool is a visualization technique that enables the comparison of the model's predicted classes against the actual ones. It provides a clear visual insight into the precision, recall, and accuracy of the predictive model, helping in understanding its effectiveness and potential areas of improvement.

On the one hand, there was some disappointment regarding the quality of the data. Although the classification accuracy exceeded 70%, it is true that there were differences due to factors such as surgery and mouse variance. After the analysis was completed, we reclassified the AI with mice that had relatively better imaging quality and were able to classify itch and pain with an accuracy of over 90%.

Despite the aforementioned limitations of the imaging itself, we confirmed through AI algorithms that neuron population responses can distinguish itch and pain signals well within the brain. SMO algorithm proved to be a robust tool for analyzing 1p calcium imaging data in the mouse ACC. I think the result contributes to the existing body of knowledge on 1p calcium imaging data analysis in mouse ACC, demonstrating the effectiveness of the SMO algorithm implemented through the Weka program. Also, the utilization of the confusion matrix as a visualization

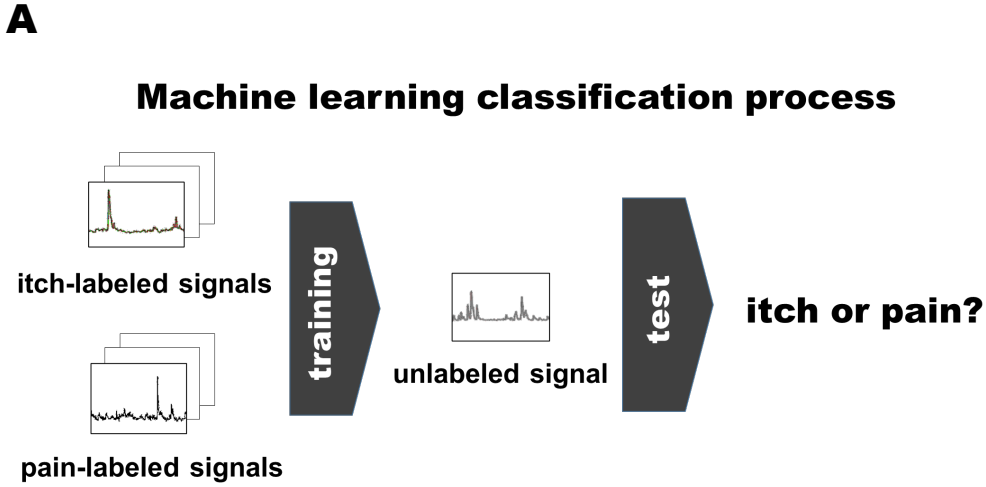

tool provided a deeper understanding of the model's predictive accuracy.

However, further research should be conducted to optimize the algorithm parameters and refine the prediction model for better accuracy and performance. If the accuracy and precision of the data improve in the future, we believe that these results can be better explained from a biological perspective. The biological factors that may influence these results include neuronal types and network topology encompassing differences in synaptic strength.

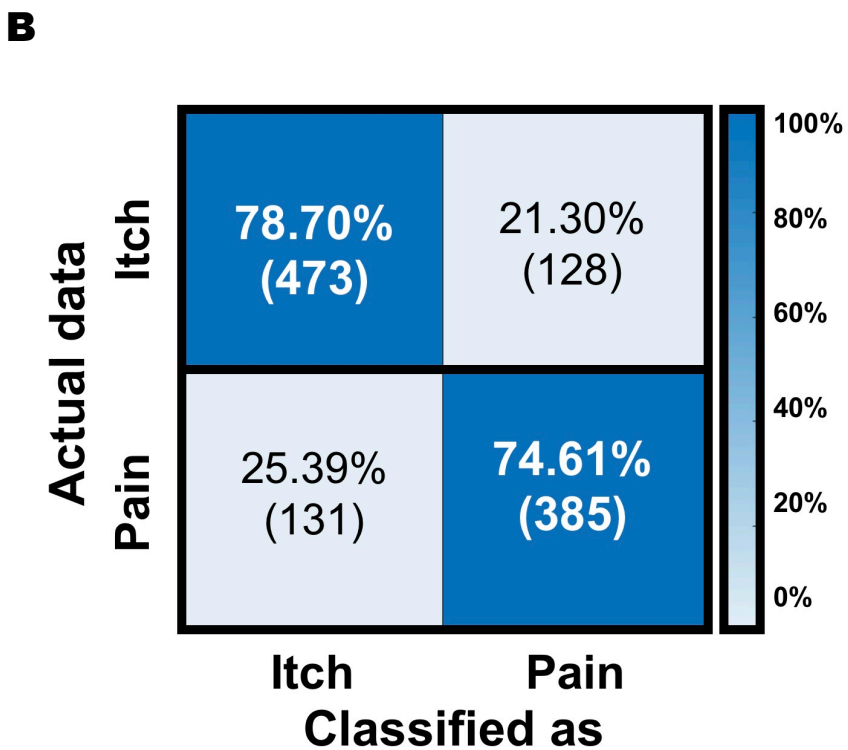

Figure 5. Machine learning classification process and classification matrix

(A) (left) overall procedure of classification process. (right) confusion matrix shows actual stimuli were classified correctly.

Chapter 4.

Itch and pain have their own network structure

Backgrounds

Although the signal analysis is a solid tool for describing itch and pain properties, I thought this analysis should be combined with network properties. In my investigation, the analysis of neuronal signaling was conducted on a single-neuron level with the expectation that an in-depth network analysis, informed by the correlations in neuronal firing, would elucidate the potential similarities and differences in the anterior cingulate cortex's (ACC's) processing of itch and pain stimuli.

The foundation for this network analysis is the cross-correlation derived from the temporal firing patterns of individual neurons, forming a type of synchrony network. Prior to embarking on the network analysis, it was essential to address a few fundamental questions regarding the nature of the proposed functional network. Specifically, it was important to ascertain whether the timing-based network analysis would indeed give rise to a functional network and how this might be influenced by the existing physical environment.

Firstly, it was imperative to investigate if the synchrony of neuronal firing was impacted by the spatial proximity of the neurons. If this effect was found to be negligible, the resultant network analysis could be interpreted as entirely functional. However, if an effect was observed, this would open the possibility of correlating the size and functionality of neuronal populations that form the itch and pain networks.First, I found itch and pain’s highly synced pair are located nearby by using physical-distance pair network analysis. (Fig 6) I found both itch and pain have unique network correlation compare to the scrambled (ramdom) network.

In order to ensure the statistical significance of certain characteristics pertaining to the network's structural and compositional properties, I employ metrics frequently utilized in mathematical network studies. The principal parameters for network analysis include the Clustering Coefficient and Average Path Length. The clustering coefficient is a quantifiable metric of the degree to which nodes within a network are interlinked, where a high clustering coefficient signifies well-clustered nodes. Moreover, the average path length is the mean distance of the shortest path across all node pairs in the network, serving as a proxy for network efficiency. For instance, a small average path length suggests rapid information propagation within the network.

Within this study, I concurrently present these two parameters, statistically characterizing them as indicators of small-world networks commonly observed in social networks, brain wiring, and internet connectivity. A characteristic feature of such networks is the simultaneous presence of a high clustering coefficient and a small average path length, resulting in a network that showcases both localized clusters and extensive global connectivity. To quantify this characteristic as small-worldness, I utilized sigma (σ), gamma (γ), and lambda (λ). Gamma (γ) is the ratio of the real network's clustering coefficient to that of the random network, and lambda (λ) is the average path length of the real network relative to the average path length of the random network. Sigma (σ), the metric representing small-worldness, is the ratio of gamma to lambda, and if σ exceeds 1, the network is considered to possess the small-world property.

Prior to these calculations, I examined the correlation, the network's fundamental parameter. I used the scrambled network as a reference point. Given

its mathematical nature, I anticipated a discrepancy from biological networks and our findings confirmed this. Intriguingly, the strength of the correlation network evolved over time, with the average correlation diminishing when pain was elicited at different time intervals using the same procedure. This implies that not all neurons detected by genetically encoded calcium indicators (GECIs) are engaged in pain processing, and as the stimulus is repeatedly introduced, a subset of neurons or their correlations become predominantly involved in pain processing.

The results derived from the small-worldness analysis were also enlightening. Small-worldness exceeded 1 in control, itch, and pain networks, indicating that the correlation network within the ACC's neuronal population is typified by high clustering and swift information processing. Furthermore, I observed a decline in small-worldness during itch and pain stimulation. As the calculation of small-worldness involves normalizing the network to a random network, this suggests the presence of distinct sub-networks within the overall network that are primarily involved in itch or pain processing, while others are relatively less engaged.

In summary, our findings indicate that the network parameters for itch and pain exhibit similarities, with pharmacologically induced itch and pain stimuli commonly leading to a reduction in small-worldness. (Fig 7,8)

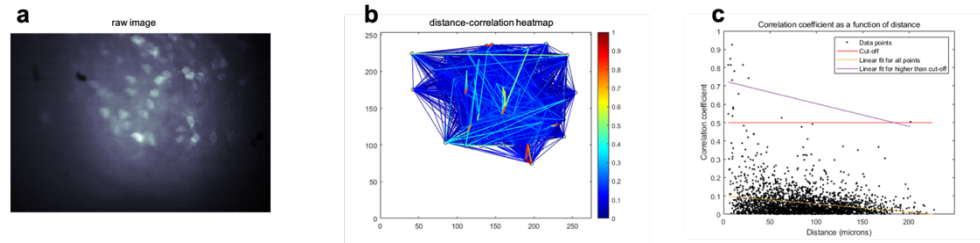

Figure 6. Physical distance and itch network property.

(a) Raw representative calcium image after histamine injection. (b) Physical distance and correlation heatmap. (c) highly correlated neurons are located nearby.

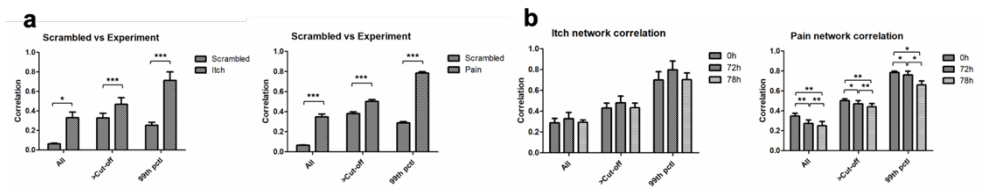

Figure 7. Network property of itch and pain network, compared with scrambled data.

(a) Scrambled vs experiment network correlation. 2-way ANOVA performed. (b) Itch and pain network correlation during 3 experiments. Mann-Whitney test performed.

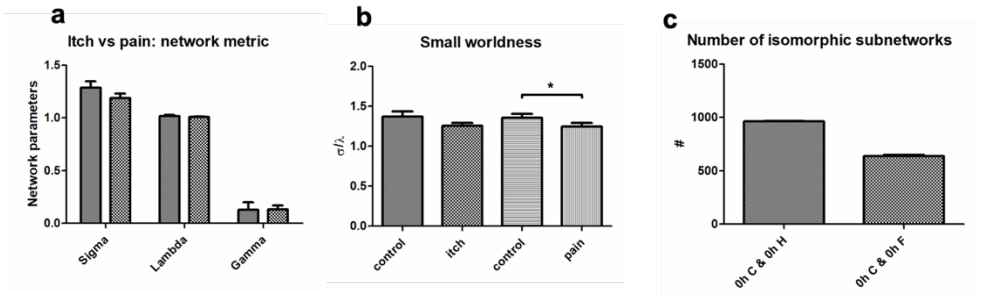

Figure 8. Network metric comparison. Small worldness difference showed pain network is affected by drug stimuli.

(a) Network metrics of itch and pain network. (b) Small worldness parameter(sigma/ lambda) comparison. Mann-Whitney test performed. (c) number of isomorphic subnetworks.

Chapter 5.

Behavior data shows itch has distinct response when mouse shows itch specific behavior

Backgrounds

The primary purpose of the experiment is to analyze whether a stimuli-specific neural population exists from the response of a cell population from stimuli. However, it would be clearer if this could be explained in relation to behavior as well. In general, a mouse responds to pain by licking and scratching to itch. Therefore, I observed the neuron population activity through a miniscope and, at the same time, tracked the behavior using a separate camera and looked at the relationship between the behavior-neuron population based on this.

For the scratching time analysis, I set a time window before and after the behavior. This allowed me to compare the average amount of fluorescent signal before scratching, during scratching, after scratching, and outside of the time window. To ensure the reliability of this data analysis, I also checked that different lengths of time windows produced similar results. In rodents, pruriceptive stimuli induce an innate behavioral response to scratching to eliminate factors that cause itchy sensations.

From the mouse behavior task, I observed cell population's peak frequency are related to two factors: 1) mouse movement 2) licking/scratching behavior. Among those two indexes, licking/scratching made more differences of cell population frequency. Also, when mouse does not show certain behavior, overall firing rate decreased as time flows.

I assumed that if there were specific neurons directly involved in the itching sensation, changes in calcium transients in this type of neuron would coincide with scratching events, as in the VLO and VTA. However, I did not find any such type

of neuron showing calcium transients synchronized with scratching bouts. In addition, this was not observed at the neuronal population level.

Next, I compared the mean calcium level 1s before and after the scratching bout. The mean calcium level decreased immediately after scratching bouts. As mentioned previously, the ACC plays a role in heterologous neurophysiological functions. Thus, I reanalyzed the internal calcium level of each neuron, which was specifically activated only after histamine injection. The results showed differences in calcium levels before and after scratching bouts, which implied that overall neuronal activity was reduced immediately after scratching. (Fig 9)

From the behavior analysis, I found that a few neurons in the ACC were accurately activated in synchronization with the scratching behavioral response. However, at the population level, the activity of ACC neurons was reduced immediately after the scratching behavioral response. Previous studies found that itch-specific neurons are activated in specific time windows of scratching behavior in the VLO and VTA. These studies were based on the assumption that scratching response is a behavioral expression of itchiness in mice. Thus, neurons that are specifically activated immediately before the scratching response can possibly mediate the itchy sensation. In this study, I did not find specific neurons showing high activities only immediately before scratching bouts. It implies that ACC may not directly elicit itchiness induced by histamine. However, apart from itchiness, pruritogens can also induce additional internal states, such as anxiety. Previous studies have shown that the ACC enhances anxiety in chronic pain condition. Thus, ACC neurons showing reduced activities immediately after scratching bouts are likely to mediate itch-induced anxiety after histamine injection. Given the hedonic

effect of scratching, it is also likely that pleasure immediately after the scratching bout suppresses ACC neurons, thereby reducing itch-induced anxiety. Another possibility is that these ACC neurons may mediate attention to the stimulus. In human and rodent, the ACC is involved in attention for cognitive and emotional process. Therefore, the scratching behavior may have distracted attention to itching stimulus by reducing the activity of these neurons. Further studies are required to fully understand these neurons showing reduced activities immediately after scratching response. The ACC is the well-known brain region in charge of multimodal function such as sensation, emotion, memory and cognition. Recently published paper shows that the medial prefrontal cortex neurons involved in remote fear memory recall are also mediate pain processing. Functional mapping has not yet been made for individual ACC neurons, but whether the itch-specific neurons of the ACC play a role in other functions, and if they do, it is also important to reveal the mechanism.

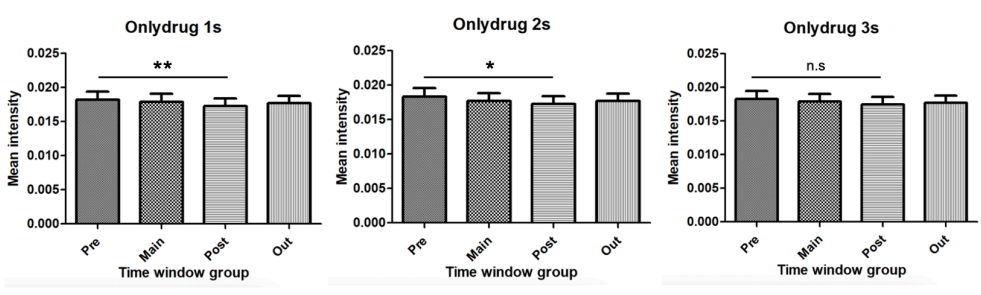

Figure 9. Time window shows pre-post Δcalcium signal efficiently.

Different time window applied (1s~3s) to calculate mean intensity. Paired t-test.

Chapter 6.

Conclusion

Conclusion

I performed novel analyses on calcium imaging data to figure out the ACC neuron population's statistical properties on itch/pain conditions.

From the PSD analysis, I found itch and pain have their frequency components. More specifically, the 0.9~5.5Hz range shows similar power distribution but not in the other range. Also, PSD distribution analysis shows itch and pain have distinct but common power bands. When I tracked triple-overlapped(which exists in all timelines), its PSD fluctuates between itch and pain's average bands. In short, itch/pain's controversial relationship could be shown at the cell level via calcium image.

By using physical-distance pair network analysis, I found itch and pain's highly synced pair are located nearby. From the network analysis, I found itch and pain have distinct network properties compared to scrambled networks. Also, the itch and pain network's time dependency was verified. The pain network showed significant correlation changes over time. Itch and pain have similar network metrics. However, pain networks have significant small worldness compared to the comparison groups.

Behavior analysis showed itch behavior can be predicted from pre-scratching signal, may imply motor related circuit is related to the ACC region.

I can suggest that, itch and pain have their own signal processing but also share a common frequency range. Itch and pain networks are dynamic, but this will be limited by the neuron's physical distance. These dynamics may explain the ACC region's multi-function with small neuron numbers.

The present study scrutinizes the phenomena of pain and itch at the level of individual neurons. The results illuminate that neurons implicated in pain and itch are distinct, can be demarcated based on their signaling, and exhibit differential network attributes. However, several subsequent steps must be executed to progress from merely analyzing these observations to comprehending the underlying principles.

Firstly, a superior level of precision or resolution in the data is mandated. Although our study faced limitations in temporal resolution due to the nature of calcium imaging, we were able to discern between pain and itch at various scales. However, these scales are not sufficient to explain the underlying mechanism in detail.

Secondly, neuronal type specificity and interpretation of structure-function relationships warrant consideration. The algorithms utilized to train the machine learning classifiers in our study were generally capable of distinguishing between pain and itch signals, despite substantial variations in their mathematical bases. Nevertheless, a biological explanation or one grounded in empirical evidence would necessitate a comprehensive understanding of individual neuron characteristics, types, locations, and connectivity.

Thirdly, additional information regarding the circuitry involved is needed. As our data constitute observations of the anterior cingulate cortex and its alterations across different experimental conditions, it is challenging to ascertain whether this region is solely implicated in the transmission of pain and itch information, or whether it is involved in computational processes such as convergence or divergence.

Incorporating these additional layers of information would enable us to grasp the essence of pain and itch processing in the anterior cingulate cortex, moving beyond the simplistic understanding of them as distinct states.

References

J. Xiu, Q. Zhang, T. Zhou, T. Zhou, Y. Chen, H. Hu, Visualizing an emotional valence map in the limbic forebrain by TAI-FISH. *Nat. Neurosci.* **17**, 1552–1559 (2014).

C. J. Han, C. M. O'Tuathaigh, L. van Trigt, J. J. Quinn, M. S. Fanselow, R. Mongeau, C. Koch, D. J. Anderson, Trace but not delay fear conditioning requires attention and the anterior cingulate cortex. *Proc. Natl. Acad. Sci.* **100**, 13087–13092 (2003).

D. Jeon, S. Kim, M. Chetana, D. Jo, H. E. Ruley, S.-Y. Lin, D. Rabah, J.-P. Kinet, H.-S. Shin, Observational fear learning involves affective pain system and Ca v 1.2 Ca 2+ channels in ACC. *Nat. Neurosci.* **13**, 482–488 (2010).

E. Valentini, The role of anterior insula and anterior cingulate in empathy for pain. *J. Neurophysiol.* **104**, 584–586 (2010).

H. Mochizuki, K. Inui, H. C. Tanabe, L. F. Akiyama, N. Otsuru, K. Yamashiro, A. Sasaki, H. Nakata, N. Sadato, R. Kakigi, Time course of activity in itch-related brain regions: a combined MEG-fMRI study. *J. Neurophysiol.* **102**, 2657–2666 (2009).

P. W. Frankland, B. Bontempi, L. E. Talton, L. Kaczmarek, A. J. Silva, The Involvement of the Anterior Cingulate Cortex in Remote Contextual Fear Memory. *Science*. **304**, 881–883 (2004).

P. W. Frankland, B. Bontempi, The organization of recent and remote memories. *Nat. Rev. Neurosci.* **6**, 119–130 (2005).

G. Bush, P. Luu, M. I. Posner, Cognitive and emotional influences in anterior cingulate cortex. *Trends Cogn. Sci.* **4**, 215–222 (2000).

T. V. P. Bliss, G. L. Collingridge, B.-K. Kaang, M. Zhuo, Synaptic plasticity in the anterior cingulate cortex in acute and chronic pain. *Nat. Rev. Neurosci.* **17**, 485–496 (2016).

K. C. Berridge, Affective valence in the brain: modules or modes? *Nat. Rev. Neurosci.* **20**, 225–234 (2019).

J.-S. Lu, Q.-Y. Chen, S. Zhou, K. Inokuchi, M. Zhuo, Dual roles of anterior cingulate cortex neurons in pain and pleasure in adult mice. *Mol. Brain*. **11**, 72 (2018).

A. J. Shackman, T. V. Salomons, H. A. Slagter, A. S. Fox, J. J. Winter, R. J. Davidson, The Integration of Negative Affect, Pain, and Cognitive Control in the Cingulate Cortex. *Nat. Rev. Neurosci.* **12**, 154–167 (2011).

L.-J. Wu, S. S. Kim, X. Li, F. Zhang, M. Zhuo, Sexual attraction enhances glutamate transmission in mammalian anterior cingulate cortex. *Mol. Brain*. **2**, 9 (2009).

J. Braz, C. Solorzano, X. Wang, A. I. Basbaum, Transmitting Pain and Itch Messages: A Contemporary View of the Spinal Cord Circuits that Generate Gate Control. *Neuron*. **82**, 522–536 (2014).

D. M. Barry, X.-T. Liu, B. Liu, X.-Y. Liu, F. Gao, X. Zeng, J. Liu, Q. Yang, S. Wilhelm, J. Yin, A. Tao, Z.-F. Chen, Exploration of sensory and spinal neurons expressing gastrin-releasing peptide in itch and pain related behaviors. *Nat. Commun.* **11**, 1397 (2020).

K. Koga, T. Chen, X.-Y. Li, G. Descalzi, J. Ling, J. Gu, M. Zhuo, Glutamate acts as a neurotransmitter for gastrin releasing peptide-sensitive and insensitive itch-related synaptic transmission in mammalian spinal cord. *Mol. Pain*. **7**, 47 (2011).

T. Liu, R.-R. Ji, New insights into the mechanisms of itch: are pain and itch controlled by distinct mechanisms? *Pflugers Arch.* **465** (2013), doi:10.1007/s00424-013-1284-2.

L. Han, C. Ma, Q. Liu, H.-J. Weng, Y. Cui, Z. Tang, Y. Kim, H. Nie, L. Qu, K. N. Patel, Z. Li, B. McNeil, S. He, Y. Guan, B. Xiao, R. H. Lamotte, X. Dong, A subpopulation of nociceptors specifically linked to itch. *Nat. Neurosci.* **16**, 174–182 (2013).

T. Akiyama, E. Carstens, in *Itch: Mechanisms and Treatment*, E. Carstens, T. Akiyama, Eds. (CRC Press/Taylor & Francis, Boca Raton (FL), 2014; http://www.ncbi.nlm.nih.gov/books/NBK200915/), *Frontiers in Neuroscience*.

S. Davidson, G. J. Giesler, The multiple pathways for itch and their interactions with pain. *Trends Neurosci.* **33**, 550–558 (2010)

G. Descalzi, T. Chen, K. Koga, X.-Y. Li, K. Yamada, M. Zhuo, Cortical GluK1 kainate receptors modulate scratching in adult mice. *J. Neurochem.* **126**, 636–650 (2013).

S. A. Josselyn, P. W. Frankland, Memory Allocation: Mechanisms and Function. *Annu. Rev. Neurosci.* **41**, 389–413 (2018).

Y. Zhou, J. Won, M. G. Karlsson, M. Zhou, T. Rogerson, J. Balaji, R. Neve, P. Poirazi, A. J. Silva, CREB regulates excitability and the allocation of memory to subsets of neurons in the amygdala. *Nat. Neurosci.* **12**, 1438–1443 (2009).

J.-H. Han, S. A. Kushner, A. P. Yiu, C. J. Cole, A. Matynia, R. A. Brown, R. L. Neve, J. F. Guzowski, A. J. Silva, S. A. Josselyn, Neuronal Competition and Selection During Memory Formation. *Science*. **316**, 457–460 (2007).

D. J. Cai, D. Aharoni, T. Shuman, J. Shobe, J. Biane, W. Song, B. Wei, M.

Veshkini, M. La-Vu, J. Lou, S. E. Flores, I. Kim, Y. Sano, M. Zhou, K. Baumgaertel, A. Lavi, M. Kamata, M. Tuszynski, M. Mayford, P. Golshani, A. J. Silva, A shared neural ensemble links distinct contextual memories encoded close in time. *Nature*. **534**, 115–118 (2016).

S. L. Commerford, A. L. Carsten, E. P. Cronkite, Histone turnover within nonproliferating cells. *Proc. Natl. Acad. Sci.* **79**, 1163–1165 (1982).

V. N. Barros, M. Mundim, L. T. Galindo, S. Bittencourt, M. Porcionatto, L. E. Mello, The pattern of c-Fos expression and its refractory period in the brain of rats and monkeys. *Front. Cell. Neurosci.* **9** (2015), doi:10.3389/fncel.2015.00072.

T.-T. Zhang, F.-Y. Shen, L.-Q. Ma, W. Wen, B. Wang, Y.-Z. Peng, Z.-R. Wang, X. Zhao, Potentiation of synaptic transmission in Rat anterior cingulate cortex by chronic itch. *Mol. Brain*. **9**, 73 (2016).

T. Akiyama, M. I. Carstens, E. Carstens, Facial Injections of Pruritogens and Algogens Excite Partly Overlapping Populations of Primary and Second-Order Trigeminal Neurons in Mice. *J. Neurophysiol.* **104**, 2442–2450 (2010).

P. W. Mantyh, S. D. Rogers, P. Honore, B. J. Allen, J. R. Ghilardi, J. Li, R. S. Daughters, D. A. Lappi, R. G. Wiley, D. A. Simone, Inhibition of hyperalgesia by ablation of lamina I spinal neurons expressing the substance P receptor. *Science*. **278**, 275–279 (1997).

E. E. Carstens, M. I. Carstens, C. T. Simons, S. L. Jinks, Dorsal horn neurons expressing NK-1 receptors mediate scratching in rats. *NeuroReport*. **21**, 303–308 (2010).

Z.-S. Han, E.-T. Zhang, A. D. Craig, Nociceptive and thermoreceptive lamina I neurons are anatomically distinct. *Nat. Neurosci.* **1**, 218–225 (1998).

J. Hachisuka, K. M. Baumbauer, Y. Omori, L. M. Snyder, H. R. Koerber, S. E. Ross, Semi-intact ex vivo approach to investigate spinal somatosensory circuits. *eLife*. **5**, e22866 (2016).

S. Davidson, X. Zhang, C. H. Yoon, S. G. Khasabov, D. A. Simone, G. J. Giesler, The Itch-Producing Agents Histamine and Cowhage Activate Separate Populations of Primate Spinothalamic Tract Neurons. *J. Neurosci.* **27**, 10007–10014 (2007).

Y.-C. Lu, Y.-J. Wang, B. Lu, M. Chen, P. Zheng, J.-G. Liu, ACC to Dorsal Medial Striatum Inputs Modulate Histaminergic Itch Sensation. *J. Neurosci.* **38**, 3823–3839 (2018).

A. J. Rashid, C. Yan, V. Mercaldo, H.-L. (Liz) Hsiang, S. Park, C. J. Cole, A. D. Cristofaro, J. Yu, C. Ramakrishnan, S. Y. Lee, K. Deisseroth, P. W. Frankland, S. A. Josselyn, Competition between engrams influences fear memory formation and recall. *Science*. **353**, 383–387 (2016).

J.-H. Han, S. A. Kushner, A. P. Yiu, H.-L. (Liz) Hsiang, T. Buch, A. Waisman, B. Bontempi, R. L. Neve, P. W. Frankland, S. A. Josselyn, Selective Erasure of a Fear Memory. *Science*. **323**, 1492–1496 (2009).

A. P. Kardon, E. Polgár, J. Hachisuka, L. M. Snyder, D. Cameron, S. Savage, X. Cai, S. Karnup, C. R. Fan, G. M. Hemenway, C. S. Bernard, E. S. Schwartz, H. Nagase, C. Schwarzer, M. Watanabe, T. Furuta, T. Kaneko, H. R. Koerber, A. J. Todd, S. E. Ross, Dynorphin Acts as a Neuromodulator to Inhibit Itch in the Dorsal Horn of the Spinal Cord. *Neuron*. **82**, 573–586 (2014).

S. J. Kang, C. Kwak, J. Lee, S.-E. Sim, J. Shim, T. Choi, G. L. Collingridge, M. Zhuo, B.-K. Kaang, Bidirectional modulation of hyperalgesia via the specific control of excitatory and inhibitory neuronal activity in the ACC. *Mol. Brain*. **8**, 81

(2015).

C. J. Nelson, S. Bonner, Neuronal Graphs: A Graph Theory Primer for Microscopic, Functional Networks of Neurons Recorded by Calcium Imaging. *Front. Neural Circuits*, (2021)

S. Malmersjö, P. Rebellato, E. Smedler, H. Planert, S. Kanatani, I. Liste, E. Nanou, H. Sunner, S. Abdelhady, S. Zhang, M. Andäng, A. E. Manira, G. Silberberg, E. Arenas, P. Uhlén, Neural progenitors organize in small-world networks to promote cell proliferation. *PNAS* (2013)

국문초록

고통 및 가려움의 회로 및 메커니즘은 주로 수용체 및 신경절에서 주로 연구되어 밀접한 관련이 있음이 알려져 있으나, 뇌 내부의 정보처리 과정에서 이 두 자극이 어떻게 구분되고 서로 영향을 주는지에 대해서는 상대적으로 잘 알려져 있지 않다. 전대상피질은 뇌 영역의 하나로 고통과 가려움 감각을 처리하는 것으로 알려져 있어, 해당 영역에서 이 두 자극을 구분하고자 하였다. 이 연구에서는 약물에 의해 유발된 고통 및 가려움 상태에서 전대상피질에 대한 1-photon 칼슘 이미지를 관찰하였다. 고통과 가려움을 표지하는 뉴런 집단들의 시간 의존성을 먼저 확인하였고, 파워 스펙트럼 밀도 분석을 기반으로 신경 발화 패턴을 분석한 결과는 고통과 가려움 자극에 따라 전대상피질이 뚜렷한 발화 패턴을 가짐을 보였다. 네트워크 분석 결과는 전대상피질에서 처리되는 고통 혹은 가려움 반응 동안 시간 의존적인 기능적 허브의 존재를 암시한다. 본 연구는 고통과 가려움 처리를 나타내는 두 개의 뉴런 집단의 존재를 밝혔다.